Original Article

http://www.jcpjournal.org
pISSN 2288-3649 · eISSN 2288-3657
https://doi.org/10.15430/JCP.2023.28.1.12

JCP

Black Tea Extract, via Modulation of TGF-β Pathway, Prevents Inorganic Arsenic-induced Development of Squamous Cell Carcinoma of the Skin in Swiss Albino Mice

Archismaan Ghosh, Madhumita Roy

Department of Environmental Carcinogenesis & Toxicology, Chittaranjan National Cancer Institute, Kolkata, India

Chronic exposure to inorganic arsenic (iAs) elevates reactive oxygen species (ROS) generation and up-regulates TGF-β signalling. This promotes induction of epithelial to mesenchymal transition (EMT) and causes the development of squamous cell carcinoma (SCC) of skin. Black tea is a popular beverage worldwide and an effective antioxidant. Chemopreventive potential of black tea extract (BTE) against iAs induced carcinogenicity has been explored here. The study aims to investigate the role of BTE in prevention of iAs-induced SCC of skin in Swiss albino mice via the modulation of TGF-β signalling and EMT. Mice were divided into (1) control, (2) iAs, (3) iAs+BTE, and (4) BTE groups and were administered iAs and BTE alone, or in combination for 330 days. Histological studies were performed to assess development of SCC. ROS generation was estimated by flowcytometry. Expression of TGF-β and downstream proteins belonging to suppressor of mothers against decapentaplegic (Smad), phosphoinositide-3-kinase (PI3K)-protein kinase B (AKT) and mitogen-activated protein kinase (MAPK) pathways was assessed by immunoblotting. Expression of EMT markers was evaluated by immunoblotting, immunohistochemistry and semi-quantitative reverse transcriptase-PCR. After 330 days of iAs treatment, development of invasive SCC of skin probably due to excess ROS generation, elevation of TGF-β, downregulation of the Smad pathway, upregulation of PI3K-AKT and MAPK signalling molecules and induction of EMT was observed. All these modulations were found to be reversed by BTE, which inhibits iAs induced SCC of skin by quenching excess ROS, promoting Smad mediated TGF-β signalling, downregulating signalling intermediates of PI3K-AKT and MAPK pathways and inhibiting EMT.

Key Words Tea, Arsenic, Transforming growth factor beta, Epithelial-mesenchymal transition, Chemoprevention

INTRODUCTION

Chronic exposure to inorganic arsenic (iAs), classified as a class 1 carcinogen by International Agency for Research on Cancer [1], causes numerous health problems [2]. Epidemiological evidence implicates chronic iAs exposure causes carcinogenesis of various organs like skin, lungs, kidney, bladder, etc. [3,4]. Drinking of iAs contaminated water is a common route of exposure to this environmental pollutant [5]. Primary symptoms of chronic iAs exposure include hyperpigmentation, hypopigmentation, keratosis, Bowen's disease, etc. These skin disorders often develop into malignancies like squamous cell carcinoma (SCC) and basal cell carcinoma [6].

Swiss albino mice chronically exposed to iAs encountered excess generation of reactive oxygen species (ROS), resulting in DNA, lipid and protein damage, induction of inflammatory cytokine production, and impairment of repair enzymes [7], as well as aberrant epigenetic modulations [8]. Excess ROS generation is linked to induction of cancer and its progression. ROS can also modulate signalling pathways by acting as secondary messengers, facilitating cell proliferation and survival [9]. One of the signalling mechanisms altered by excess ROS generation involves the pathway, where the downstream molecules like suppressor of mothers against decapentaplegic (Smad), mitogen-activated protein kinase (MAPK), and NF-κB are modulated, leading to increased cell motility [10]. TGF-β on the other hand can induce excess ROS generation, as well as help maintain high levels of ROS within the system by impairing the activity of antioxidants [11].

Received January 18, 2023, Revised February 2, 2023, Accepted February 4, 2023
Correspondence to Madhumita Roy, E-mail: mitacnci@yahoo.co.in, https://orcid.org/0000-0002-3551-8534

ROS and TGF-β are interdependent and both can regulate levels of each other [12]. TGF-β, which is implicated in tumorigenesis, may play a dual role. TGF-β acts as a tumor suppressor and a growth inhibitor in normal cells and early stages of tumorigenesis; but in later stages, it acts as a growth promoter, inducing epithelial to mesenchymal transition (EMT), invasion and metastasis [13]. EMT, a phenomenon where transition of epithelial to mesenchymal cells takes place, is involved in embryogenesis, wound healing, and cancer progression [14]. EMT results in loss of cell-cell contact due to downregulation of junctional complex proteins (claudins, zonula occludens, and E-cadherin) and desmosomal proteins (desmoplakin, desmoglein, etc.) [15,16]. Loss of apical-basal polarity of the cells with simultaneous upregulation of Vimentin and rearrangement of the actin filaments also takes place during this period [17]. All these modifications promote the invasive characteristics of the cells leading to metastasis.

TGF-β mediates its downstream signalling through canonical and non-canonical pathways. Canonically, TGF-β transfers its signals by Smad2 or Smad3. Smad2/3 is phosphorylated by TGF-β receptor 1 (TGF-βR1), resulting in formation of a heteromeric complex with Smad4. This Smad2/3-Smad4 complex migrates to the nucleus and alters gene transcription [18]. Contrastingly in a non-canonical pathway, TGF-β can activate the phosphoinositide-3-kinase (PI3K)-protein kinase B (AKT), as well as MAPK signalling [13]. Reports show that TGF-β induces EMT via the canonical pathway through overactivation of Smad3 and Smad4 [19]. On the contrary, another study indicates Smad2 and Smad3 to be inhibitors of EMT; therefore, loss of Smad2 promotes EMT, hence skin carcinogenesis [20]. Activation of PI3K is linked to induction of EMT via rearrangement of actin filaments and increased cell migration [15]. In mammary epithelial cells and keratinocytes, phosphorylated AKT activated mTOR complex 1 (mTORC1) and ribosomal S6 kinase (S6K), resulting in enhanced protein synthesis followed by increased motility and invasion [21].

TGF-β also activates mTORC2, which promotes reorganisation of the actin cytoskeleton, Ras homolog family member A activation and cell migration, ultimately promoting EMT. mTORC2 can also activate AKT forming a positive feedback loop for the PI3K-AKT pathway [22]. TGF-β, upon binding to its receptors, can also activate the c-Jun N-terminal kinases (JNK) and p38 MAPK [23]. This growth factor induces lysine-63 linked polyubiquitination at lysine-34 of TGF-β-associated kinase 1 (TAK1) by TNF receptor-associated factor 6, which leads to TAK-1 activation [24]. TAK1, a member of MAPK kinase kinase (MAPKKK) family, activates its downstream MAPK kinases 3/4 (MAPKK3/4) which further activates JNK and p38 MAPK [23]. Phosphorylation of TAK1 induces activation and nuclear translocation of NF-κB, activating pro-survival signalling [24]. TGF-β triggers activation of JNK and p38 MAPK, which promotes EMT by inducing cytoskeletal rearrangement [23]. Therefore, TGF-β may induce EMT via both canonical (Smad) and non-canonical (PI3K-AKT and MAPK) pathways, promoting cancer metastasis.

EMT is a key player in carcinogenesis; therefore, inhibition of EMT may be an effective approach to cancer prevention and treatment [25]. Excess ROS generation triggers TGF-β-induced EMT [26]; therefore, quenching of ROS may be an alternative effective strategy of cancer control. Phytochemicals, by virtue of their antioxidative potential [27], may quench ROS, eliciting a chemopreventive role. Black tea, one of the most popular beverages, exhibits pronounced antioxidative properties [28] by inhibiting/scavenging free radicals. Report from our laboratory showed that black tea extract (BTE) effectively quenched iAs- induced ROS production [7], and mitigated epigenetic modulations, preventing carcinogenesis in Swiss albino mice [8]. BTE was found to inhibit iAs-induced EMT in skin keratinocyte (HaCaT) cells, thus exhibiting its chemopreventive potential in an in vitro model [29]. BTE, by virtue of its antioxidant potential, may prevent iAs-induced EMT in Swiss albino mice.

MATERIALS AND METHODS

Materials

Acrylamide, N,N′-methylenebis-acrylamide, and RETROscript (reverse transcriptase [RT]-PCR kit; Ambion; ThermoFisher Scientific) were procured from Invitrogen BioServices India Pvt. Ltd. Taq-polymerase was procured from HiMedia. Ethidium bromide (EtBr), agarose, sodium arsenite ($NaAsO_2$), diaminobenzidine (DAB), 2′,7′-dichlorofluorescin diacetate, and bovine serum albumin were obtained from Sigma-Aldrich. Goat Immunoglobulin G anti-rabbit and anti-mouse (alkaline phosphatase conjugated and horseradish peroxidase conjugated) were purchased from Genetex; 5-bromo-4-chloro-3-indolyl phosphate/nitro blue tetrazolium (BCIP-NBT) was bought from Santa Cruz Biotechnology; nitrocellulose membrane was purchased from GE HealthCare; Glycine, Tris and SDS were purchased from Amresco. Primary antibodies anti-TGF-β, anti-Smad2 (phospho [p]Ser467), anti-Smad3 (pSer423/425), anti-phosphatase and tensin homolog deleted on chromosome 10 (PTEN), anti-PI3Kp110α, anti-AKT (pSer473), anti-mTOR, anti-S6Kp70, anti-NF-κB/p65, anti-TAK1 (pThr184), anti-MAPKK3 (pSer189), anti-p38 MAPK, anti-MAPKK4 (pThr 261), anti-JNK, anti-E-cadherin, anti-desmoplakin, anti-vimentin, anti-N-cadherin, anti-Snail, anti-Slug, anti-Twist, anti-β-actin, and anti-Zeb1 were purchased from Genetex. Anti-Smad4 (pThr277) was purchased from ThermoFischer Scientific.

Methods

1) Animal maintenance

Male Swiss albino mice (*Mus musculus*), aged around 4–5 weeks, were obtained from Chittaranjan National Cancer Institute. Ethical approval was provided by the Institutional

Animal Ethics Committee (IAEC approval number: 1774/MR-3/2017/9), which was validated by Committee for the Purpose of Control and Supervision of Experiments on Animals, New Delhi. Handling of the mice and experimentations were carried out following Animal Research Reporting of in Vivo Experiments (ARRIVE) protocols. Synthetic food pellets were fed to the mice along with water ad libitum. The mice were kept alternately in light and darkness (12 hours in each condition), to maintain optimum conditions, with an ambient temperature of 22 ± 2°C. Experimental mice were maintained at the same height from the ground, to provide identical living environment. To obtain tissues for experimental purposes, the mice were sacrificed using overdose of thiopentone sodium (100 mg/kg body weight).

2) Animal treatment

The experimental animals (Swiss albino mice) were divided into four groups with 25 mice in each group; 5 mice were placed in each cage. To remove the hair, mice were shaved in their hind leg region with a razor. The groups were as follows:

(1) Group 1: control group, where the mice were given normal food pellets and tap water.

(2) Group 2: iAs treated group, where the mice were given sodium arsenite (500 μg/L) dissolved in water, as the only source of drinking water. Mice were painted in the shaven hind leg region with the same concentration of iAs.

(3) Group 3: iAs + BTE treated mice group, where the mice were given sodium arsenite (500 μg/L) contaminated water. Their shaved skin was also painted with the same concentration of iAs. These mice were also given lyophilized BTE at a concentration of 0.33 mg/g body weight via oral gavage, thrice daily (an interval of 8 hours).

(4) Group 4: BTE group, where the mice were given normal food pellets and tap water, along with BTE (0.33 mg/g body weight). BTE was administered thrice daily, i.e., 8 hourly. Previous studies showed that BTE elicited no effect; therefore, results have not been given.

After 330 days, mice were sacrificed as described above and the tissues were collected.

3) Preparation of BTE

BTE administered to mice was prepared according to the standard laboratory protocol [8].

4) Isolation of leukocytes

In order to isolate the leukocytes, blood samples collected from the mice were mixed with Solution A (0.87% NH_4Cl in 10 mM Tris-HCl, pH: 7.2) in the ratio 1:3 and incubated at 0°C for 20–30 minutes, followed by centrifugation at 400 *g* for 20 minutes at 0°C. The pellet obtained was mixed with solution A and centrifuged at 400 *g* for 10 minutes. The resultant pellet was suspended in solution B (0.25 M mesoinositol, 10 mM sodium phosphate, and 1 mM $MgCl_2$, pH: 7.2).

5) ROS estimation using flowcytometry

The isolated leukocytes were pelleted down by centrifugating at 1,500 rpm for 5 minutes and suspended in hydroxyethyl piperazine ethane sulfonicacid (HEPES) buffered saline (HBS; consisting of 140 mM HCl, 5 mM KCl, 10 mM HEPES, 1 mM $CaCl_2$, 1 mM $MgCl_2$, and 10 mM glucose). The leukocyte suspension was pelleted and resuspended in HBS, following which 10 μM of dichloro-dihydro-fluorescein diacetate (DCFH-DA) was added and incubated in the dark for 45 minutes. After the incubation period, the leukocyte suspension was pelleted and resuspended in HBS to remove excess of DCFH-DA. Flowcytometric analysis of the ROS was performed by using the DxFLEX flow cytometer (Beckman Coulter Life Sciences).

6) Immunoblot assay

Proteins from tissues were quantitated by the Bradford's Reagent. The assay was performed according to the protocol, as mentioned by Sarkars et al [30]. Equal quantities of proteins were loaded into each well and electrophoresed in SDS polyacrylamide gels. They were then electroblotted unto a nitrocellulose membrane and incubated overnight at 4°C with primary antibody (1:1,000). After incubation, the membrane was washed to remove excess primary antibody, followed by incubation at 4°C for 2 hours with secondary antibody. BCIP-NBT was used for staining. The bands obtained were quantified by the software Image Master™ 17 2D Elite, version 3.1 (GE HealthCare).

7) Immunohistochemistry (IHC)

IHC was performed on paraffin embedded formalin fixed tissues [8]. Primary antibodies were added in the ratio 1:500 and incubated overnight at 4°C. Horseradish peroxidase (HRP) tagged secondary antibodies were added in the ratio of 1:1,000 and incubated for 40 minutes at room temperature. DAB was used as a substrate for HRP. The tissues were mounted in Dibutylphthalate Polystyrene Xylene and observed under a bright field microscope. Images were captured at ×400. Minimum of 50 fields for each point were analysed. The quantification of the staining was performed according to the conventional scoring system [31], where stained cells (%) are classified into 6 percentage scores (PS) based on staining intensity and observation fields are classified into 4 intensity scores (IS). The PS and the IS have been shown in the Table 1, 2 respectively. Final Allred Score (AS) is calculated as the sum of percentage score and intensity score, AS = PS + IS. The following table lists the PS and IS.

8) Semi-quantitative reverse transcriptase (RT)-PCR analysis

TRIzol reagent (guanidine thiocyanate and phenol) was used to isolate RNA from the animal tissues. The purity of RNA was assessed using a nanodrop-spectrophotometer (Nabi; MicroDigital Co.,Ltd). Two micrograms of extracted RNA

Table 1. Table showing percentage score (PS)

Percentage of stained cells	PS
0	0
<1	1
1–10	2
11–33	3
34–66	4
≥67	5

The percentage of stained cells observed in each field has been dived into different ranges and numbers have been assigned to each category for calculation of the final Allred score.

Table 2. Table showing Intensity score (IS)

Intensity of staining	IS
None	0
Weak	1
Intermediate	2
Strong	3

The intensity of staining of each field observed under microscope has been divided into four groups and number are assigned to each category for the calculation of the final Allred score.

was converted to cDNA using a RETROscript kit (Ambion; ThermoFischer Scientific). The cDNAs were then subjected to amplification by PCR using respective forward and reverse primers. The primer sequences used for the amplification are as follows.

E-cadherin
Forward primer = 5'-GGCTTCAGTTCCGAGGTCT-3'
Reverse primer = 5'-GAAAAGAAGGCTGTCCTTGG-3'
Desmoplakin
Forward primer = 5'- TCAACGACCAGAACTCCGAC-3'
Reverse primer = 5'-TTTGCAGCATTTCTTGGATGG-3'
Vimentin
Forward primer = 5'-AAAGCACCCTGCAGTCATTC-3'
Reverse primer = 5'-AGCCACGCTTTCATACTGCT-3'
N-cadherin
Forward primer = 5'-AAGGACAGCCCCTTCTCAAT-3'
Reverse primer = 5'-CTGGCTCGCTGCTTTCATAC-3'
Snail
Forward primer = 5'-CACCCTCATCTGGGACTCTC-3'
Reverse primer = 5'-AGGTGGACGAGAAGGACGAC-3'
Slug
Forward primer = 5'-AACATTTCAACGCCTCCAAG-3'
Reverse primer = 5'-TGAACCACTGTGATCCTTGG-3'
Twist
Forward primer = 5'-CGGACAAGCTGAGCAAGATT-3'
Reverse primer = 5'-CCAGACGGAGAAGGCGTAG-3'
Zeb1
Forward primer = 5'-CCAAGAACTGCTGGCAAGA-3'
Reverse primer = 5'-GATAAATGACGGCGGTGTCT-3'

The PCR products were subjected to electrophoresis in 2% agarose gel, stained with EtBr. After electrophoresis, the gel was viewed in ChemiDoc XRS + Imaging system (BioRad) and the band intensities were documented.

9) Statistical analysis

Statistical analysis was performed using IBM SPSS Statistics software version 22.0 (IBM Corp.). One-way ANOVA Tukey Test was performed to evaluate the statistical significance of the different experimental groups. $P < 0.001$ has been considered to be significant and $P < 0.0001$ has been considered to be highly significant.

RESULTS

Development of SCC of the skin in Swiss albino mice and its prevention

After a treatment period of 330 days, iAs treated mice developed invasive lesions on the skin, which were confirmed histologically to be invasive SCC (data not given). Contrastingly, the iAs + BTE treated mice developed only few lesions which were mostly hyperplasic and dysplastic in nature. These results indicate that BTE inhibits iAs induced skin carcinogenesis. This data has already been published from our laboratory [8]. To understand the preventive mechanism of BTE in iAs-induced SCC, detailed investigation was carried out.

Enhancement of ROS generation upon chronic iAs exposure and its amelioration by BTE

ROS generated in the leukocytes have been estimated by Flowcytometric analysis, and representative histograms are depicted in Figure 1A. Histogram of the iAs treated mice clearly shows a prominent right shift of the peak indicating higher percentage of ROS generating cells (85.4%) than the control mice (8.12%). Histogram of the iAs + BTE treated mice shows an effective left shift of the peak, with respect to the iAs treated mice, suggesting a lower percentage of ROS generating cells (42.6%). The bar graph represented in Figure 1B shows the mean percentages of ROS generating cells in the control, iAs and iAs + BTE. The results suggest that upon chronic exposure to iAs, there is a significant ($P < 0.0001$) increase in ROS whereas intervention with BTE significantly ($P < 0.0001$) reduces the proportion of ROS generating cells in Swiss albino mice. Previous studies from our group showed that a specific free radical scavenger N-acetyl-L-cysteine attenuated the elevated level of ROS [32], which supports our present finding.

Modulation of the TGF-β pathway upon chronic iAs exposure and its amelioration by BTE

Expression of TGF-β and its downstream signalling proteins have been assessed by the immunoblotting assay at 330 days of treatment. Lanes 1, 2, and 3 denote the control, iAs, and iAs + BTE groups respectively. Representative immunoblots are depicted in Figure 2A. Fold changes in band intensities of proteins have been represented by a bar graph in Figure 2B. From these figures, it is evident that the

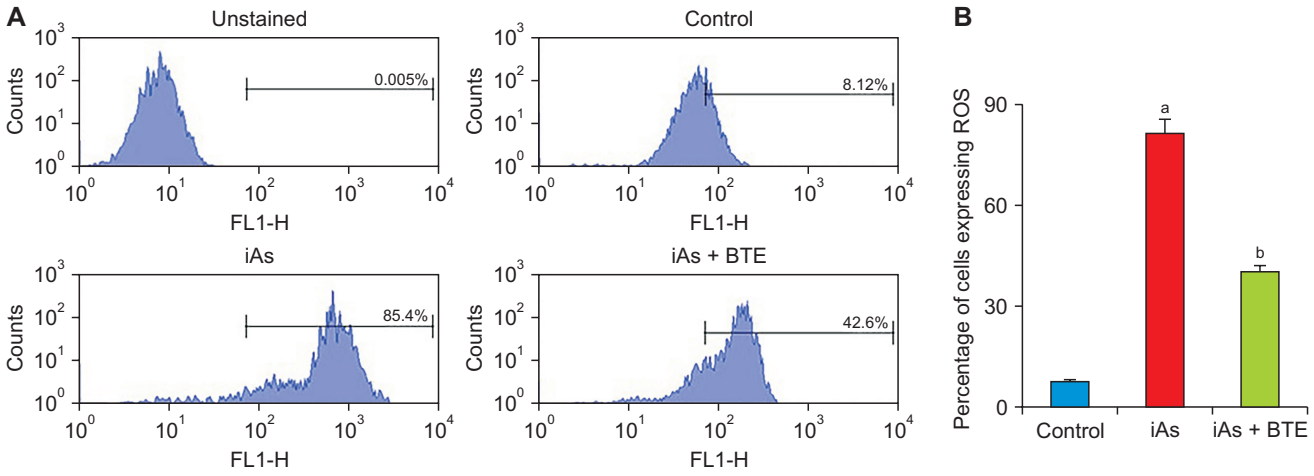

Figure 1. Effects of BTE on iAs-induced ROS generation. Leukocytes isolated from the blood of the Swiss albino mice, belonging to control, iAs and iAs + BTE treatment groups, were stained with 2′,7′-dichlorofluorescin diacetate and subjected to flowcytometric analysis to detect ROS generation after 330 days of treatment. (A) displays histograms representing the percentage of ROS generating cells. The histogram of iAs treated mice shows a prominent right shift of the fluorescence channel-1 peak with respect to the control, indicating excess ROS generation. Histogram peak of iAs + BTE treated mice shows a left shift, compared to the iAs treated mice, suggesting quenching of ROS. The proportions of leukocytes expressing ROS in the control, iAs and iAs + BTE treated mice are 8.12%, 85.4%, and 42.6%, respectively. (B) displays a bar graph indicating the mean percentages of ROS generating cells in the control, iAs and iAs + BTE treated mice. The experiments have been performed thrice and representative histograms are displayed. ROS, reactive oxygen species; iAs, inorganic arsenic; BTE, black tea extract. The increase in mean percentage of ROS generating cells in the iAs treated mice is significant at $^{a}P < 0.0001$, compared to the control mice. The decrease in the mean percentages of ROS generating cells in the iAs + BTE treated mice is significant at $^{b}P < 0.0001$, with respect to iAs treated mice.

expression of TGF-β has been upregulated significantly ($P < 0.0001$) in the iAs treated mice compared to the control. In the iAs + BTE treated mice, the change in the expression of TGF-β is insignificant ($P = 0.065$) compared to the iAs group. These results suggest that the expression of TGF-β increases upon chronic iAs exposure, while BTE fails to modulate it. In the tissues of the iAs treated mice, pSmad2 and pSmad3 showed significant ($P < 0.001$), and pSmad4 showed more significant ($P < 0.0001$) downregulation, with respect to the control group. Contrastingly, the expression of pSmad2 and pSmad3 was found to be significantly ($P < 0.001$) higher, and upregulation of pSmad4 was highly significant ($P < 0.0001$) in the iAs + BTE treated mice, with respect to the iAs group. This indicates that the Smad pathway (canonical) remains active in the iAs + BTE group, while it is effectively downregulated upon chronic iAs exposure.

Appreciable ($P < 0.0001$) upregulation of PI3Kp110α and pAKT, and significant ($P < 0.0001$) downregulation of PTEN, an inhibitor of the PI3K-AKT pathway, were observed in the iAs treated mice. This indicates activation of the PI3K-AKT pathway, one of the non-canonical pathways through which TGF-β transduces its downstream signalling. In iAs + BTE administered mice, the expression of PTEN is significantly ($P < 0.001$) higher and that of PI3Kp110α and pAKT is significantly ($P < 0.0001$) lower than in the iAs treated mice, hinting at downregulation of the PI3K-AKT pathway. Downstream molecular targets of the PI3K-AKT pathway such as mTOR, S6K and NF-κB/p65 are also significantly ($P < 0.0001$) enhanced in the iAs treated mice. In iAs + BTE treated group, mTOR, S6K ($P < 0.0001$) and NF-κB/p65 ($P < 0.001$) are significantly downregulated. All these results suggest that TGF-β transmits its downstream signalling via activation of the PI3K-AKT pathway and its downstream effector molecules in mice chronically exposed to iAs. Activity of PI3K-AKT and its effector molecules are downregulated in iAs + BTE treated mice.

The band intensities of the MAPK pathway show that in iAs treated mice, there is highly significant ($P < 0.0001$) upregulation of pTAK1, pMAPKK3, pMAPKK4, p38 MAPK and JNK1/2. In the iAs + BTE treated mice, the expression of pTAK1, pMAPKK3, pMAPKK4 and p38 MAPK was significantly ($P < 0.0001$) downregulated. Expression of JNK1/2 has also been downregulated by BTE ($P < 0.001$). Results indicate that upon chronic exposure to iAs, TGF-β can also transmit its signalling along the (non-canonical) MAPK pathway through activation of TAK-1 and its downstream effector molecules. In the iAs + BTE treated mice, the signalling mediators of the MAPK pathway are appreciably downregulated, indicating that TGF-β acts mainly via the Smad pathway. β-Actin was used as loading control.

Induction of of EMT upon chronic iAs administration and its amelioration by BTE

Representative immunoblots showing the expression of EMT markers at 330 days of treatment are depicted in Figure 3A. Fold changes in band intensities of EMT proteins have been represented as a bar graph in Figure 3C. The numbers 1, 2, and 3 represent control, iAs, and iAs + BTE treated mice, respectively in Figure 3A. From Figure 3A and 3C, it can be

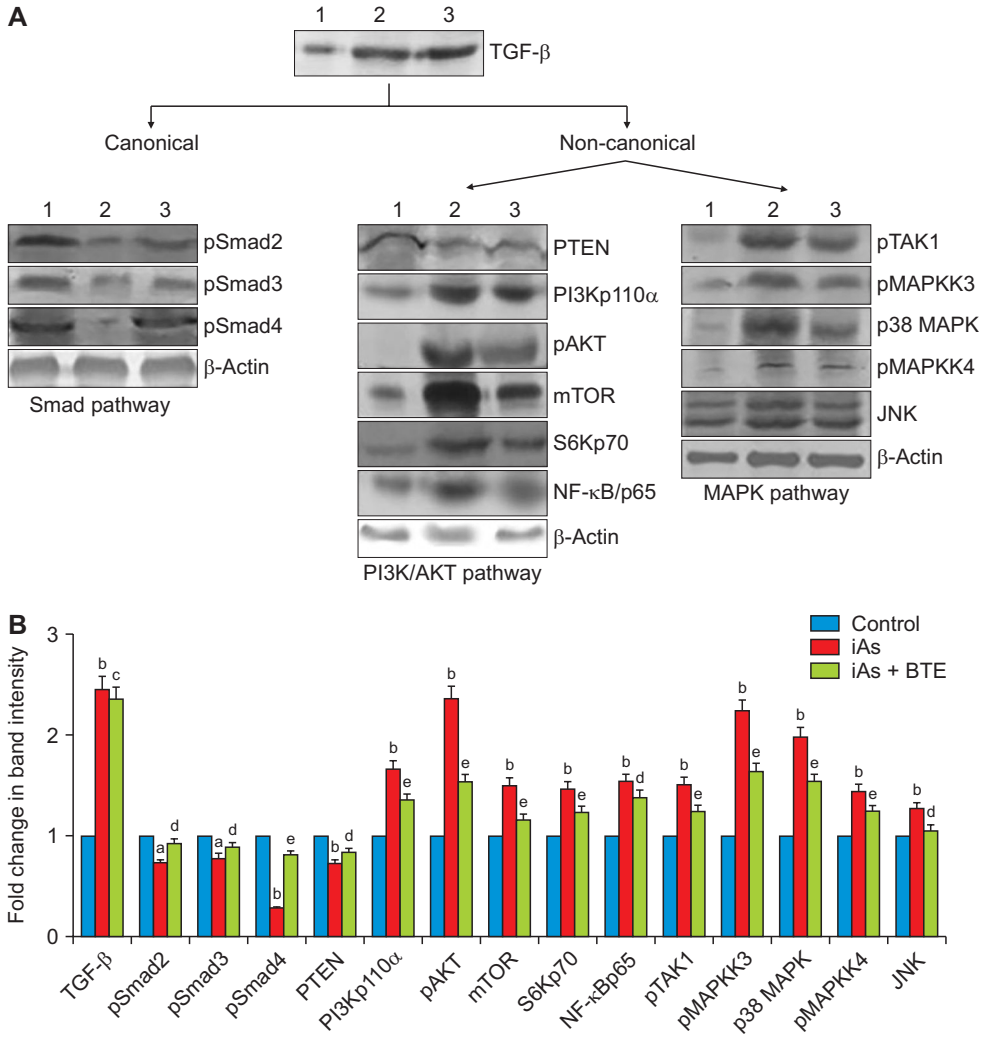

Figure 2. Investigation of the canonical and non-canonical pathways of TGF-β in iAs treated mice and its modulation by BTE. The results after 330 days of treatment, suggests that TGF-β mostly transmits its downstream signalling non-canonically, via the PI3K-AKT and MAPK pathways in iAs treated mice whereas in the iAs + BTE treated mice, TGF-β acts primarily via the canonical Smad pathway, and signalling intermediates of the PI3K-AKT and MAPK pathways were downregualted. (A) displays representative immunoblot bands of TGF-β and its downstream signalling proteins, belonging to Smad, PI3K-AKT and MAPK pathways. β-Actin has been used as the loading control. The lanes 1, 2, and 3 represent control, iAs and iAs + BTE treated Swiss albino mice, respectively. (B) shows the fold change in mean band intensities of TGF-β and its downstream signalling proteins in a bar graph. Results are expressed as mean of three independent experiments ± standard deviation. PI3K-AKT, phosphoinositide-3-kinase-protein kinase B; iAs, inorganic arsenic; BTE, black tea extract; Smad, suppressor of mothers against decapentaplegic; PTEN, phosphatase and tensin homolog deleted on chromosome 10; PI3K, phosphoinositide-3-kinase; AKT, protein kinase B; S6K, S6 kinase; TAK, TGF-β-associated kinase; MAPK, mitogen-activated protein kinase; MAPKK, MAPK kinases; JNK, c-Jun N-terminal kinase; p, phospho. Modulation of TGF-β expression and its down stream signalling proteins in the iAs treated mice, in comparison to the control mice, is significant at $^{a}P < 0.001$ and highly significant at $^{b}P < 0.0001$. Alteration in expression of TGF-β and its downstream signalling proteins, in the iAs + BTE treated mice, in comparison to the iAs treated mice, is insignificant at $^{c}P = 0.065$, significant at $^{d}P < 0.001$, and highly significant at $^{e}P < 0.0001$.

seen that upon chronic exposure to iAs, expression of epithelial markers like E-cadherin and desmoplakin has been significantly ($P < 0.0001$) reduced in comparison to control mice. Simultaneously, the expression of mesenchymal protein markers like vimentin, N-cadherin, Snail, Slug, Twist, and Zeb1 has been significantly ($P < 0.0001$) increased with respect to control mice. Therefore, chronic iAs exposure leads to reduction of epithelial markers and gain of mesenchymal markers in Swiss albino mice. In iAs + BTE administered mice, expression of E-cadherin ($P < 0.0001$) and that of desmoplakin ($P < 0.001$) are significantly upregulated compared to the iAs treated mice, suggesting gain of epithelial characteristics by BTE. The expression of mesenchymal proteins is significantly ($P < 0.0001$) downregulated, indicative of loss of mesenchymal characteristics. Results indicate that BTE prevents reduction of epithelial factors and gain of mesenchymal factors, hindering EMT.

Representative images of the Semi-quantitative RT-PCR

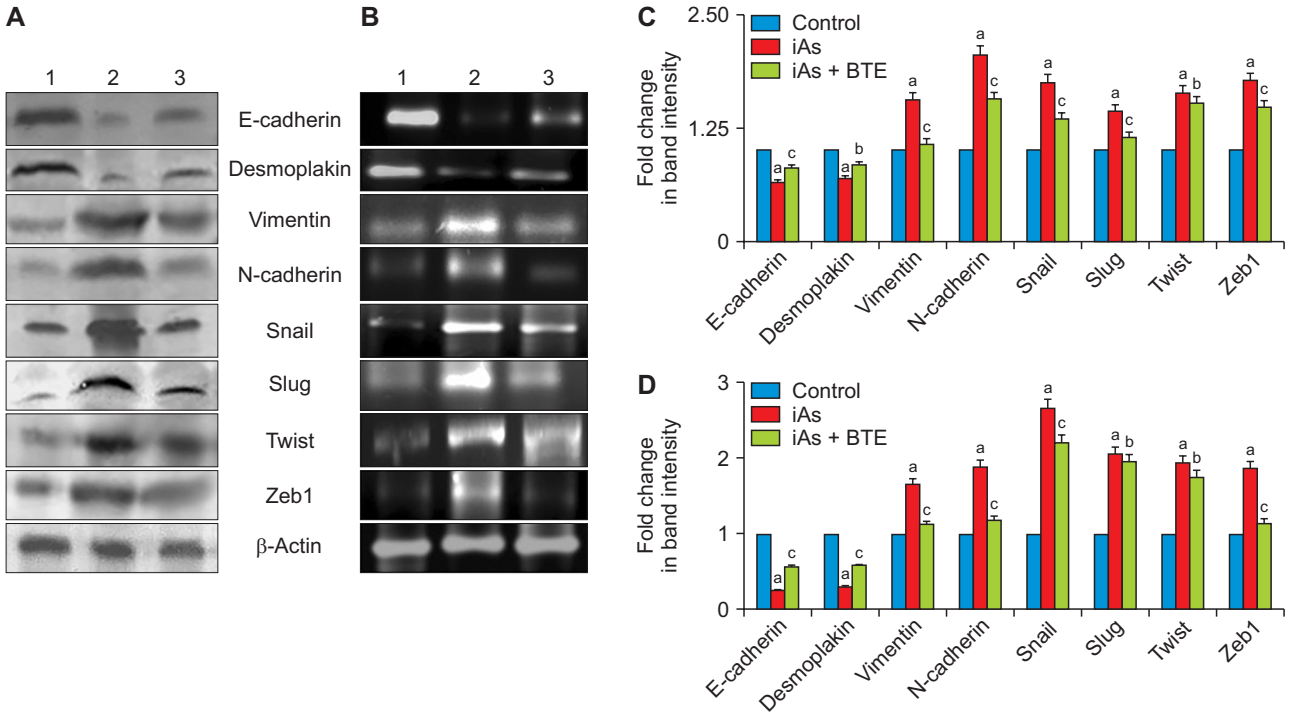

Figure 3. Effects of BTE on iAs-induced EMT. After 330 days of treatment, the results show downregulation of epithelial markers (E-cadherin and desmoplakin) and upregulation of mesenchymal markers (vimentin, N-cadherin, Snail, Slug, Twist, and Zeb1) in the iAs treated mice, at the protein and mRNA levels; while in the iAs + BTE treated mice, these results were reversed. (A) displays representative Immunoblot bands of the respective EMT markers. The lanes 1, 2, and 3 represent control, iAs, and iAs + BTE treated mice respectively. β-Actin is the loading control. (B) displays representative RT-PCR bands of the respective EMT markers. (C) displays a bar graph representing fold change in band intensities of the immunoblots of respective EMT markers. The results are expressed as mean of three independent experiments ± standard deviation. EMT, epithelial to mesenchymal transition; RT-PCR, reverse transcriptase PCR; iAs, inorganic arsenic; BTE, black tea extract. The modulation of the EMT markers in the iAs treated mice tissues, with respect to the control mice, is highly significant at $^{a}P < 0.0001$. The alteration of EMT markers in the iAs + BTE treated mice, with respect to the iAs treated mice, is significant at $^{b}P < 0.001$ and highly significant at $^{c}P < 0.0001$. (D) shows a bar graph representing the fold change in RT-PCR band intensities of the respective EMT markers. The alteration in PCR bands of respective EMT markers in the iAs treated mice, with respect to the control group, is highly significant at $^{a}P < 0.0001$. The modulation of bands in the iAs + BTE treated mice, with respect to the iAs treated mice, is significant at $^{b}P < 0.001$ and highly significant at $^{c}P < 0.0001$.

blots of respective epithelial and mesenchymal markers are shown in the Figure 3B. The fold changes in band intensity of PCR blots have been shown by bar graph in Figure 3D. The numbers 1, 2, and 3 represent the control, iAs, and iAs + BTE groups, respectively. From Figure 3B and 3D, it can be clearly seen that band intensities of the PCR products of the epithelial markers were significantly ($P < 0.0001$) decreased while that of the mesenchymal markers was significantly ($P < 0.0001$) increased in Swiss albino mice, when chronically exposed to iAs. This finding is in line with our immunoblot results. This is indicative of the fact that iAs causes downregulation of epithelial markers and simultaneous upregulation of mesenchymal markers with respect to the control mice. The PCR products and band intensities of iAs + BTE treated mice show significant ($P < 0.0001$) upregulation of epithelial markers. Significant downregulation ($P < 0.001$) of mesenchymal proteins has been achieved with BTE. The results indicate inhibition of iAs induced EMT by BTE. Thus, BTE can prevent iAs-induced progression of EMT by upregulating the epithelial markers, and downregulating the mesenchymal markers, both at the protein and mRNA levels, thereby exhibiting its anticancer potential.

Assessment of the expression of EMT markers via IHC

The expression of EMT markers in the formalin fixed tissue sections of control iAs and iAs + BTE treated Swiss albino mice was measured by IHC. The representative IHC images of the respective EMT markers are depicted in Figure 4. Semi-quantitative analysis of IHC was performed following the AS system. The AS of the respective EMT markers of each treatment group (control, iAs, and iAs + BTE) is listed in Table 3. According to AS, upon chronic exposure to iAs, there is an effective downregulation of epithelial proteins and upregulation of the mesenchymal proteins, supporting the immunoblot results of EMT markers. The AS indicates that chronic iAs exposure has an important role in induction of EMT in Swiss albino mice. The AS of the iAs + BTE treated mice display enhancement and diminution of the epithelial and mesenchymal markers, with respect to the iAs treated

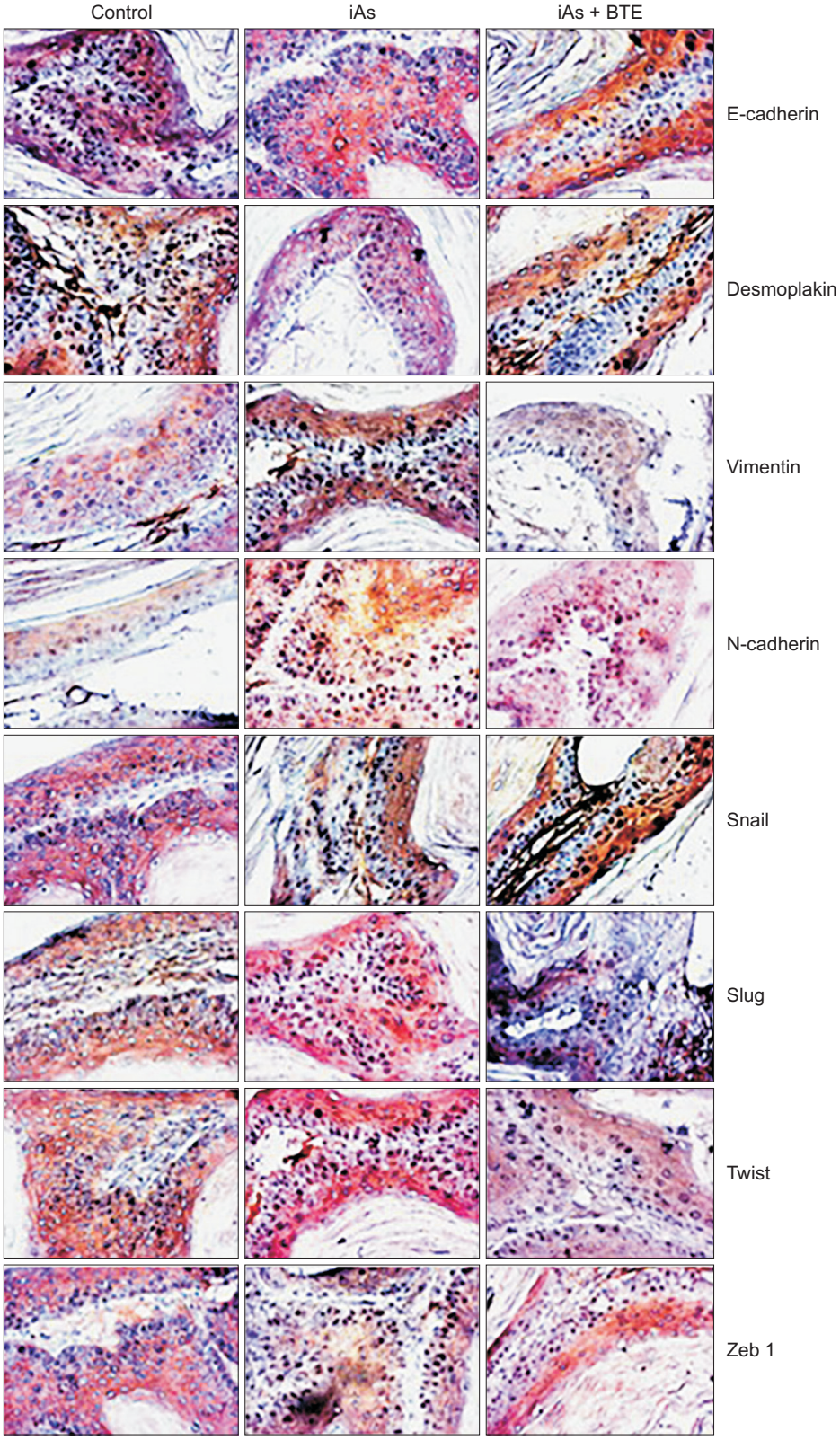

Figure 4. Assessment of EMT marker expression by IHC. Representative IHC images of the respective EMT markers in control, iAs, and iAs + BTE treated mice have been displayed. The results suggest downregulation of epithelial markers (E-cadherin and desmoplakin) and upregulation of mesenchymal markers (vimentin, N-cadherin, Snail, Slug, Twist, and Zeb1) in iAs treated mice and its reversal in iAs + BTE treated mice. IHC was performed on formalin fixed, paraffin embedded, mouse skin tissues, which after incubating with antibodies, were stained with diaminobenzidine. Images were captured with a bright field microscope at ×400. Fifty fields were analyzed for each marker from each treatment group and representative photographs for epithelial and mesenchymal markers are depicted. iAs, inorganic arsenic; BTE, black tea extract; IHC, immunohistochemistry; EMT, epithelial to mesenchymal transition.

Table 3. Allred score for immunohistochemistry of the respective EMT markers

EMT markers	Control	iAs	iAs + BTE
E-cadherin	8 ± 0.36	3 ± 0.09[a]	5 ± 0.11[b]
Desmoplakin	7 ± 0.24	4 ± 0.18[a]	6 ± 0.17[b]
Vimentin	2 ± 0.12	7 ± 0.30[a]	4 ± 0.20[b]
N-cadherin	1 ± 0.03	6 ± 0.25[a]	4 ± 0.08[b]
Snail	4 ± 0.18	8 ± 0.28[a]	5 ± 0.23[b]
Slug	3 ± 0.11	8 ± 0.33[a]	6 ± 0.25[c]
Twist	2 ± 0.08	6 ± 0.18[a]	4 ± 0.18[b]
Zeb	3 ± 0.12	7 ± 0.22[a]	4 ± 0.05[b]

Values are presented as mean ± standard deviation. Allred score of the respective EMT markers of the control, iAs and iAs + BTE treated mice has been tabulated. EMT, mesenchymal transition; iAS, inorganic arsenic; BTE, black tea extract. [a]Significant at $P < 0.0001$ with respect to control group of mice. Significant at [b]$P < 0.0001$ and [c]$P < 0.001$ with respect to the iAs group of mice.

mice. This reiterates our immunoblot and PCR results.

DISCUSSION

Chronic exposure to iAs for 330 days led to the development of SCC in the skin of Swiss albino mice; whereas BTE intervention elicited a protective effects. Histological analysis revealed that the lesions developed by iAs treatment were mostly invasive carcinomas, while those mild lesions seen in iAs + BTE treated mice were only dysplastic in nature [8]. The present study focuses on elucidation of the mechanistic pathways involved in the development of invasive SCC of the skin, vis a vis the preventive role brought about by the administration of BTE.

The present investigation shows that excess ROS generation is a direct consequence of chronic iAs exposure. Excess ROS may prompt initiation and development of cancer. ROS may also act as signalling intermediates engaged in cell proliferation, angiogenesis, EMT and metastasis [33]. iAs exposure to HaCaT cells led to excess ROS generation and induction of EMT [29]. Higher expression of TGF-β has been found in iAs treated group of mice, compared to the control group. This is indicative of the fact that there may be a correlation between high ROS generation and elevated expression of TGF-β.

ROS has been reported to promote EMT via modulation of the TGF-β pathway, ultimately leading to cancer [26]. Our present study shows that in the iAs + BTE treated mice, ROS generation was quenched substantially; however, the expression of TGF-β remains unaltered, indicating that BTE failed to modulate its expression. In the iAs treated mice, prominent downregulation of pSmad2, pSmad3 and pSmad4 was found, indicating downregulation of the canonical TGF-β signalling cascade. Suppressed expression of pSmad2, pSmad3 and pSmad4 due to chronic iAs exposure got upregulated by BTE intervention, suggesting that BTE keeps the canonical pathway active. Smad4 is considered to be a tumor suppressor, and loss of Smad4 has been highly implicated in SCC of skin, head and neck cancer [34]. Downregulation of Smad4 in the iAs treated mice may be linked to the development of SCC of the skin in mice, which may be prevented by BTE.

Downregulation of PTEN and upregulation of PI3K, AKT, mTOR, S6K and NF-κB/p65 indicate that TGF-β in iAs treated mice may have transmitted its downstream signalling via the PI3K-AKT cascade. PTEN is a tumor suppressor protein and is known to inhibit AKT. It downregulates the activation of mTOR and other downstream molecular mediators of AKT [35]. Downregulation of PTEN, in the iAs treated mice, may be responsible for the development of carcinoma. Phosphorylated AKT activates mTOR, which further forms mTORC1 and acts along with S6K to promote cell motility and invasion [21]. Activated mTOR can also form mTORC2 which leads to cytoskeletal rearrangement, promoting invasive movement of the cells [22]. Phosphorylation of AKT is reported to stabilize NF-κB/p65 and aids in its translocation to the nucleus. Thus, cell proliferation is facilitated along with evasion of apoptosis [36].

Phosphorylated AKT leads to stabilization and activation of transcription factors like Snail and Twist which promote EMT [37,38]. Overactivation of the PI3K-AKT pathway has been observed in SCC, and downregulation of AKT along with its associated signalling molecules has given promising results in skin cancer treatment [39,40]. According to a study, activation of mTOR by TGF-β led to development of EMT-like characteristics in a human breast epithelial cell line. These transformed cells showed stemness and drug resistance potential [41]. Therefore, it may be inferred that TGF-β guided activation of the PI3K-AKT pathway may promote EMT and induction of SCC of skin in iAs treated mice.

Immunoblot results show that the MAPK pathway was also active in the iAs treated mice. Activation of TAK1 (MAPKKK) led to the activation of MAPKK3 and MAPKK4 which further upregulated the expression of p38MAPK and JNK1/2, respectively. Upregulation of TAK1 in various carcinomas of the gastric, oesophageal, thyroid, and ovarian origin as well as in osteosarcoma has been reported [42]. TAK1 promotes the nuclear localisation of NF-κB/p65, which in turn promotes activation of Cyclin D1 and alters cell proliferation [42]. Therefore, cell proliferation may be boosted via upregulation of TAK1.

Upregulation of p38 MAPK has also been implicated in tumor promotion. Activation of p38 MAPK due to application of mechanical stress in pancreatic cancer cells led to promotion of EMT and cell migration [43]. An association between high level of p38 MAPK and EMT had been documented in mammary epithelial cells, exhibiting cancer stem cell characteristics and metastatic properties. Knockdown of p38 MAPKα led to inhibition of EMT even when transcription factors like Snail and Twist were upregulated, indicating the relevance of p38 MAPK in tumorigenesis [44]. Upregulation of p38 MAPKγ

enhanced the ability of breast cancer cells to form spheroid, indicating enhancement of stem cell like properties in them [45].

Upregulation of JNK1/2 was found to promote EMT by the activation of Snail and Twist in KB epithelial carcinoma cell line. Downregulation of JNK1/2 resulted in inhibition of EMT and migratory properties of the cancer cells [46]. In gastric cancer cells, inhibition of JNK resulted in halting of EMT and inhibition of migratory properties. Both p38 MAPK and JNK seem to be very potent inducers of EMT [47]. Activation of p38 MAPK and JNK has also been reported in UV-induced SCC of skin and inhibition of their activation resulted in repression of cancer progression [48].

In the present study, TGF-β appears to be transmitting its downstream signalling via the MAPK pathway along with the PI3K-AKT signalling cascade in iAs treated mice. Signalling intermediates of these pathways can promote and regulate transcription factors which induce mesenchymal features within the tissue, aiding in EMT. In the iAs + BTE group, no substantial activation of signalling intermediates, of both PI3K-AKT and MAPK pathways, has been found, suggesting downregulation of the non-canonical TGF-β pathway in them. Majority of the downstream TGF-β signalling cascade in iAs + BTE treated mice might have followed the canonical Smad pathway. Therefore, we may say that BTE supresses signalling molecular intermediates of the PI3K-AKT and MAPK pathways.

The expression of EMT markers was assessed both at the protein (by immunoblotting and IHC) the mRNA (by semi-quantitative RT-PCR) levels. The results clearly indicate that upon chronic exposure of iAs, there is significant suppression of epithelial markers like E-cadherin and desmoplakin and prominent elevation of mesenchymal markers like vimentin, N-cadherin, Snail, Slug, Twist and Zeb1. This is suggestive of the fact that down- and up-regulation of epithelial and mesenchymal markers in iAs treated mice is due to modulation at the translational transcriptional levels. Upon BTE intervention, expression of the epithelial markers is quite high while that of mesenchymal markers is low, indicating inhibition of EMT.

A previous study from our laboratory found BTE to be a potential antioxidant which was not only able to quench excess ROS generated due to chronic iAs exposure, but was also able to prevent DNA, protein and lipid damages, upregulate DNA repair enzymes, activate antioxidative enzymes and inhibit pro-inflammatory cytokine secretions in Swiss albino mice [7]. Similar observations have been reported in in vitro studies, where BTE showed its potential to reverse EMT and repress cell migration in human oral carcinoma cells (SCC4) [25]. BTE was also found to inhibit chronic iAs-induced cell transformation and induction of EMT in HaCaT cells [29]. BTE also elicits a prominent role in preventing iAs-induced epigenetic modulations in Swiss albino mice, exhibiting its chemopreventive potential [8]. Present findings indicate that excess generation of ROS was effectively quenched due to thevantioxidative activity of BTE. BTE also exhibited a vital role in down-regulating the signalling intermediates of PI3K-AKT and MAPK pathways like AKT, mTOR, JNK, and p38 MAPK which are potential inducers of EMT. Smad2, 3, and 4 were found to be active in BTE administered mice suggesting that majority of TGF-β signalling was transmitted via the canonical pathway. Upregulation of the tumor suppressor protein Smad4 upon BTE administration highlights its chemopreventive potential. BTE showed its ability to control EMT by modulating the responsible proteins, at both the protein and mRNA levels.

In conclusion, it may be inferred that chronic exposure to iAs generates ROS, induces non-canonical TGF-β signalling (activation of PI3K-AKT and MAPK pathway) and promotes EMT which culminates in SCC of skin in Swiss albino mice. Contrastingly, administration of BTE quenches excess ROS generation, promotes TGF-β signalling via the Smad pathway, anddownregulates signalling intermediates of PI3K-AKT and MAPK pathways, which are implicated in EMT, thereby inhibiting the phenomenon. Therefore, BTE may be used as a chemopreventive agent to counter iAS-induced SCC of the skin. Further studies in human population, chronically exposed to iAs, are warranted to establish the clinical potential of BTE.

ACKNOWLEDGEMENTS

The authors would like to acknowledge Director, Chittaranjan National Cancer Institute (CNCI), Kolkata and Ministry of Health and Family Welfare, India. for financial and infrastructural support.

FUNDING

This study was funded from the intramural institute fund provided by Ministry of Health and Family Welfare, India.

CONFLICTS OF INTEREST

No potential conflicts of interest were disclosed.

ORCID

Archismaan Ghosh, https://orcid.org/0000-0001-8756-2820
Madhumita Roy, https://orcid.org/0000-0002-3551-8534

REFERENCES

1. Zhou Q, Xi S. A review on arsenic carcinogenesis: epidemiology, metabolism, genotoxicity and epigenetic changes. Regul Toxicol Pharmacol 2018;99:78-88.
2. Huang HW, Lee CH, Yu HS. Arsenic-induced carcinogenesis and immune dysregulation. Int J Environ Res Public Health

2019;16:2746.
3. Sawada N. [Association between arsenic intake and cancer-from the viewpoint of epidemiological study]. Nihon Eiseigaku Zasshi 2018;73:265-8. Japanese.
4. Smith AH, Marshall G, Roh T, Ferreccio C, Liaw J, Steinmaus C. Lung, bladder, and kidney cancer mortality 40 years after arsenic exposure reduction. J Natl Cancer Inst 2018;110:241-9.
5. Abdul KS, Jayasinghe SS, Chandana EP, Jayasumana C, De Silva PM. Arsenic and human health effects: a review. Environ Toxicol Pharmacol 2015;40:828-46.
6. Hunt KM, Srivastava RK, Elmets CA, Athar M. The mechanistic basis of arsenicosis: pathogenesis of skin cancer. Cancer Lett 2014;354:211-9.
7. Ghosh A, Mukherjee S, Roy M. Chemopreventive role of black tea extract in Swiss albino mice exposed to inorganic arsenic. Asian Pac J Cancer Prev 2021;22:3647-61.
8. Ghosh A, Lahiri A, Mukherjee S, Roy M, Datta A. Prevention of inorganic arsenic induced squamous cell carcinoma of the skin in Swiss albino mice by black tea through epigenetic modulation. Heliyon 2022;8:e10341.
9. Glasauer A, Chandel NS. Targeting antioxidants for cancer therapy. Biochem Pharmacol 2014;92:90-101.
10. Krstić J, Trivanović D, Mojsilović S, Santibanez JF. Transforming growth factor-beta and oxidative stress interplay: implications in tumorigenesis and cancer progression. Oxid Med Cell Longev 2015;2015:654594.
11. Ishikawa F, Kaneko E, Sugimoto T, Ishijima T, Wakamatsu M, Yuasa A, et al. A mitochondrial thioredoxin-sensitive mechanism regulates TGF-β-mediated gene expression associated with epithelial-mesenchymal transition. Biochem Biophys Res Commun 2014;443:821-7.
12. Chung J, Huda MN, Shin Y, Han S, Akter S, Kang I, et al. Correlation between oxidative stress and transforming growth factor-beta in cancers. Int J Mol Sci 2021;22:13181.
13. Baba AB, Rah B, Bhat GR, Mushtaq I, Parveen S, Hassan R, et al. Transforming growth factor-beta (TGF-β) signaling in cancer-a betrayal within. Front Pharmacol 2022;13:791272.
14. Kim DH, Xing T, Yang Z, Dudek R, Lu Q, Chen YH. Epithelial mesenchymal transition in embryonic development, tissue repair and cancer: a comprehensive overview. J Clin Med 2017;7:1.
15. Lamouille S, Xu J, Derynck R. Molecular mechanisms of epithelial-mesenchymal transition. Nat Rev Mol Cell Biol 2014;15:178-96.
16. Huang Z, Zhang Z, Zhou C, Liu L, Huang C. Epithelial-mesenchymal transition: the history, regulatory mechanism, and cancer therapeutic opportunities. MedComm (2020) 2022;3:e144.
17. Datta A, Deng S, Gopal V, Yap KC, Halim CE, Lye ML, et al. Cytoskeletal dynamics in epithelial-mesenchymal transition: insights into therapeutic targets for cancer metastasis. Cancers (Basel) 2021;13:1882.
18. Clayton SW, Ban GI, Liu C, Serra R. Canonical and noncanonical TGF-β signaling regulate fibrous tissue differentiation in the axial skeleton. Sci Rep 2020;10:21364.
19. Vincent T, Neve EP, Johnson JR, Kukalev A, Rojo F, Albanell J, et al. A SNAIL1-SMAD3/4 transcriptional repressor complex promotes TGF-beta mediated epithelial-mesenchymal transition. Nat Cell Biol 2009;11:943-50.
20. Rose AM, Spender LC, Stephen C, Mitchell A, Rickaby W, Bray S, et al. Reduced SMAD2/3 activation independently predicts increased depth of human cutaneous squamous cell carcinoma. Oncotarget 2018;9:14552-66.
21. Lamouille S, Derynck R. Cell size and invasion in TGF-beta-induced epithelial to mesenchymal transition is regulated by activation of the mTOR pathway. J Cell Biol 2007;178:437-51.
22. Lamouille S, Connolly E, Smyth JW, Akhurst RJ, Derynck R. TGF-β-induced activation of mTOR complex 2 drives epithelial-mesenchymal transition and cell invasion. J Cell Sci 2012;125(Pt 5):1259-73.
23. Zhang YE. Non-smad signaling pathways of the TGF-β family. Cold Spring Harb Perspect Biol 2017;9:a022129.
24. Hamidi A, von Bulow V, Hamidi R, Winssinger N, Barluenga S, Heldin CH, et al. Polyubiquitination of transforming growth factor β (TGFβ)-associated kinase 1 mediates nuclear factor-κB activation in response to different inflammatory stimuli. J Biol Chem 2012;287:123-33.
25. Chang YC, Chen PN, Chu SC, Lin CY, Kuo WH, Hsieh YS. Black tea polyphenols reverse epithelial-to-mesenchymal transition and suppress cancer invasion and proteases in human oral cancer cells. J Agric Food Chem 2012;60:8395-403.
26. Lu Q, Wang WW, Zhang MZ, Ma ZX, Qiu XR, Shen M, et al. ROS induces epithelial-mesenchymal transition via the TGF-β1/PI3K/Akt/mTOR pathway in diabetic nephropathy. Exp Ther Med 2019;17:835-46.
27. Ranjan A, Ramachandran S, Gupta N, Kaushik I, Wright S, Srivastava S, et al. Role of phytochemicals in cancer prevention. Int J Mol Sci 2019;20:4981.
28. Sinha D, Roy S, Roy M. Antioxidant potential of tea reduces arsenite induced oxidative stress in Swiss albino mice. Food Chem Toxicol 2010;48:1032-9.
29. Ghosh A, Mukherjee S, Roy M. Black tea extract prevents inorganic arsenic induced uncontrolled proliferation, epithelial to mesenchymal transition and induction of metastatic properties in HaCaT keratinocytes - an in vitro study. Toxicol In Vitro 2022;85:105478.
30. Sarkars R, Mukherjee S, Roy M. Targeting heat shock proteins by phenethyl isothiocyanate results in cell-cycle arrest and apoptosis of human breast cancer cells. Nutr Cancer 2013;65:480-93.
31. Allred DC, Harvey JM, Berardo M, Clark GM. Prognostic and predictive factors in breast cancer by immunohistochemical analysis. Mod Pathol 1998;11:155-68.
32. Sarkar R, Mukherjee S, Biswas J, Roy M. Phenethyl isothiocyanate, by virtue of its antioxidant activity, inhibits invasiveness and metastatic potential of breast cancer cells: HIF-1α as a putative target. Free Radic Res 2016;50:84-100.
33. Aggarwal V, Tuli HS, Varol A, Thakral F, Yerer MB, Sak K, et al. Role of reactive oxygen species in cancer progression:

molecular mechanisms and recent advancements. Biomolecules 2019;9:735.
34. Hernandez AL, Young CD, Wang JH, Wang XJ. Lessons learned from SMAD4 loss in squamous cell carcinomas. Mol Carcinog 2019;58:1648-55.
35. Georgescu MM. PTEN tumor suppressor network in PI3K-Akt pathway control. Genes Cancer 2010;1:1170-7.
36. Akca H, Demiray A, Tokgun O, Yokota J. Invasiveness and anchorage independent growth ability augmented by PTEN inactivation through the PI3K/AKT/NFkB pathway in lung cancer cells. Lung Cancer 2011;73:302-9. Erratum in: Lung Cancer 2016;101:147.
37. Xue G, Restuccia DF, Lan Q, Hynx D, Dirnhofer S, Hess D, et al. Akt/PKB-mediated phosphorylation of Twist1 promotes tumor metastasis via mediating cross-talk between PI3K/Akt and TGF-β signaling axes. Cancer Discov 2012;2:248-59.
38. Julien S, Puig I, Caretti E, Bonaventure J, Nelles L, van Roy F, et al. Activation of NF-kappaB by Akt upregulates Snail expression and induces epithelium mesenchyme transition. Oncogene 2007;26:7445-56.
39. Mercurio L, Albanesi C, Madonna S. Recent updates on the involvement of PI3K/AKT/mTOR molecular cascade in the pathogenesis of hyperproliferative skin disorders. Front Med (Lausanne) 2021;8:665647.
40. Hwang SY, Chae JI, Kwak AW, Lee MH, Shim JH. Alternative options for skin cancer therapy via regulation of AKT and related signaling pathways. Int J Mol Sci 2020;21:6869.
41. Harvey RF, Pöyry TAA, Stoneley M, Willis AE. Signaling from mTOR to eIF2α mediates cell migration in response to the chemotherapeutic doxorubicin. Sci Signal 2019;12:eaaw6763.
42. Mukhopadhyay H, Lee NY. Multifaceted roles of TAK1 signaling in cancer. Oncogene 2020;39:1402-13.
43. Kalli M, Li R, Mills GB, Stylianopoulos T, Zervantonakis IK. Mechanical stress signaling in pancreatic cancer cells triggers p38 MAPK- and JNK-dependent cytoskeleton remodeling and promotes cell migration via Rac1/cdc42/Myosin II. Mol Cancer Res 2022;20:485-97.
44. Kudaravalli S, den Hollander P, Mani SA. Role of p38 MAP kinase in cancer stem cells and metastasis. Oncogene 2022;41:3177-85.
45. Xu M, Wang S, Wang Y, Wu H, Frank JA, Zhang Z, et al. Role of p38γ MAPK in regulation of EMT and cancer stem cells. Biochim Biophys Acta Mol Basis Dis 2018;1864:3605-17.
46. Zhan X, Feng X, Kong Y, Chen Y, Tan W. JNK signaling maintains the mesenchymal properties of multi-drug resistant human epidermoid carcinoma KB cells through snail and twist1. BMC Cancer 2013;13:180.
47. Choi Y, Ko YS, Park J, Choi Y, Kim Y, Pyo JS, et al. HER2-induced metastasis is mediated by AKT/JNK/EMT signaling pathway in gastric cancer. World J Gastroenterol 2016;22:9141-53.
48. Zhang J, Bowden GT. Activation of p38 MAP kinase and JNK pathways by UVA irradiation. Photochem Photobiol Sci 2012;11:54-61.